Electronic Supplementary Material to: "Gravity-driven coatings on curved substrates: a differential geometry approach"

Pier Giuseppe Ledda[1,2]†, M. Pezzulla [3], E. Jambon-Puillet [4], P-T Brun [4] and F. Gallaire[1]

[1]Laboratory of Fluid Mechanics and Instabilities, École Polytechnique Fédérale de Lausanne, CH-1015 Lausanne, Switzerland

[2]Dipartimento di Ingegneria Civile, Ambientale e Architettura, University of Cagliari, 09123 Cagliari, Italy

[3]Slender Structures Lab, Department of Mechanical and Production Engineering, Århus University, Inge Lehmanns Gade 10, 8000 Århus C, Denmark

[4]Department of Chemical and Biological Engineering, Princeton University,Princeton, New-Jersey 08540, USA

1. Parametrization, metric and curvature tensor for different substrates

1.1. *Monge parameterization of a generic substrate*

In the *Monge parameterization*, the substrate height is described through the function

$$\boldsymbol{X} = (x, y, h^0(x, y)), \tag{1.1}$$

i.e. the parameters that describe the surface are the x and y directions themselves, ($x^{\{1\}} = x, x^{\{2\}} = y$). This form is convenient when the substrate thickness is known as a function of the global reference frame, and fails when the substrate cannot be represented as a function of (x, y), e.g. in the case of vertical tangent.

The derivatives of the height function $h^0(x, y)$ read:

$$\begin{gathered} h^0_{(1,0)} = \partial_x h^0, \quad h^0_{(0,1)} = \partial_y h^0 \\ h^0_{(2,0)} = \partial_x \partial_x h^0, \quad h^0_{(1,1)} = \partial_x \partial_y h^0, \quad h^0_{(0,2)} = \partial_y \partial_y h^0 \end{gathered} \tag{1.2}$$

The tangent and normal vectors to the substrate are:

$$\begin{gathered} \mathbf{e}_1 = \partial_1 \boldsymbol{X} = \left[1, 0, h^0_{(1,0)}\right], \quad \mathbf{e}_2 = \partial_2 \boldsymbol{X} = \left[0, 1, h^0_{(0,1)}\right], \\ \mathbf{e}_3 = \frac{\mathbf{e}_1 \times \mathbf{e}_2}{|\mathbf{e}_1 \times \mathbf{e}_2|} = \frac{\mathbf{e}_1 \times \mathbf{e}_2}{n} = \frac{1}{n}[-h^0_{(1,0)}, -h^0_{(0,1)}, 1] \end{gathered} \tag{1.3}$$

The covariant vectors are found solving the linear system for the i-th covariant vector $\mathbf{e}^{\{i\}} \cdot \mathbf{e}_j = \delta_{ij},\ i, j = 1, 2, 3$. Note that $\mathbf{e}^{\{3\}} = \mathbf{e}_3$, since the normal-to-the-substrate vector is normalized by construction. The metric tensor and the inverse metric tensor therefore read:

† Email address for correspondence: pier.ledda@epfl.ch

$$\mathbb{G}_{ij} = \mathbf{e}_i \cdot \mathbf{e}_j = \begin{pmatrix} 1 + \left(h^0_{(1,0)}\right)^2 & h^0_{(1,0)} h^0_{(0,1)} \\ h^0_{(1,0)} h^0_{(0,1)} & 1 + \left(h^0_{(0,1)}\right)^2 \end{pmatrix},$$
$$\mathbb{G}^{\{ij\}} = \mathbf{e}^{\{i\}} \cdot \mathbf{e}^{\{j\}} = \frac{1}{n^2} \begin{pmatrix} 1 + \left(h^0_{(0,1)}\right)^2 & -h^0_{(1,0)} h^0_{(0,1)} \\ -h^0_{(1,0)} h^0_{(0,1)} & 1 + \left(h^0_{(1,0)}\right)^2 \end{pmatrix}. \tag{1.4}$$

The curvature tensor reads:

$$\mathbb{K}_i^{\{j\}} = \frac{1}{n^3} \begin{pmatrix} \left(1 + \left(h^0_{(0,1)}\right)^2\right) h^0_{(2,0)} - h^0_{(1,0)} h^0_{(0,1)} h^0_{(1,1)} & \left(1 + \left(h^0_{(1,0)}\right)^2\right) h^0_{(1,1)} - h^0_{(1,0)} h^0_{(0,1)} h^0_{(2,0)} \\ \left(1 + \left(h^0_{(0,1)}\right)^2\right) h^0_{(1,1)} - h^0_{(1,0)} h^0_{(0,1)} h^0_{(0,2)} & \left(1 + \left(h^0_{(1,0)}\right)^2\right) h^0_{(0,2)} - h^0_{(1,0)} h^0_{(0,1)} h^0_{(1,1)} \end{pmatrix}, \tag{1.5}$$

from which the mean and Gaussian curvature are obtained:

$$\begin{aligned} \mathcal{K} &= \frac{1}{n^3} \left(\left(1 + \left(h^0_{(0,1)}\right)^2\right) h^0_{(2,0)} - 2 h^0_{(1,0)} h^0_{(0,1)} h^0_{(1,1)} + \left(1 + \left(h^0_{(1,0)}\right)^2\right) h^0_{(0,2)} \right) \\ \mathcal{G} &= \frac{1}{n^4} \left(h^0_{(2,0)} h^0_{(0,2)} - \left(h^0_{(1,1)}\right)^2 \right) \end{aligned} \tag{1.6}$$

The gravity vector, which reads $\boldsymbol{g} = [0, 0, -1]$ in the (x, y, z) coordinate system, is projected on the contravariant base:

$$\begin{aligned} g_t^{\{1\}} &= \boldsymbol{g} \cdot \mathbf{e}^{\{1\}} = -h^0_{(1,0)}/n^2, \\ g_t^{\{2\}} &= \boldsymbol{g} \cdot \mathbf{e}^{\{2\}} = -h^0_{(0,1)}/n^2, \\ g_3 &= \boldsymbol{g} \cdot \mathbf{e}_3 = -1/n. \end{aligned} \tag{1.7}$$

These equations close the lubrication model.

1.2. *Monge parameterization of a surface of revolution*

A cylindrical reference frame (r, φ, z) is introduced. In this case, the Monge parameterization assumes the form:

$$\boldsymbol{X} = (r \cos\varphi, r \sin\varphi, h^0(r)). \tag{1.8}$$

The tangent and normal to the substrate vectors are

$$\begin{aligned} \mathbf{e}_1 = \mathbf{e}_r = \partial_r \boldsymbol{X} = [\cos\varphi, \sin\varphi, h^{0\prime}], \quad \mathbf{e}_2 = \mathbf{e}_\varphi = \partial_\varphi \boldsymbol{X} = [-r\sin\varphi, r\cos\varphi, 0], \\ \mathbf{e}_3 = [-h^{0\prime}\cos\varphi, -h^{0\prime}\sin\varphi, 1]. \end{aligned} \tag{1.9}$$

The covariant vectors are found solving the linear system for the ith covariant vector $\mathbf{e}^{\{i\}} \cdot \mathbf{e}_j = \delta_{ij},\ i, j = 1, 2, 3$. As before, the metric tensor and the inverse metric tensor are evaluated:

$$\mathbb{G}_{ij} = \mathbf{e}_i \cdot \mathbf{e}_j = \begin{pmatrix} 1 + \left(h^{0\prime}\right)^2 & 0 \\ 0 & r^2 \end{pmatrix}, \quad \mathbb{G}^{\{ij\}} = \mathbf{e}^{\{i\}} \cdot \mathbf{e}^{\{j\}} = \begin{pmatrix} \frac{1}{1+\left(h^{0\prime}\right)^2} & 0 \\ 0 & 1/r^2 \end{pmatrix}. \quad (1.10)$$

The curvature tensor thus reads:

$$\mathbb{K}_i^{\{j\}} = \frac{1}{\sqrt{1 + \left(h^{0\prime}\right)^2}} \begin{pmatrix} \frac{-h^{0\prime\prime}}{1+\left(h^{0\prime}\right)^2} & 0 \\ 0 & -h^{0\prime}/r \end{pmatrix}, \quad (1.11)$$

from which the mean and Gaussian curvature are obtained:

$$\mathcal{K} = \mathrm{Tr}(\mathbb{K}), \quad \mathcal{G} = \mathrm{Det}(\mathbb{K}). \quad (1.12)$$

Considering the gravity direction $\boldsymbol{g} = [0, 0, -1]$, the components along the coordinate vectors read:

$$\begin{aligned} g_t^{\{1\}} &= \boldsymbol{g} \cdot \mathbf{e}^{\{1\}} = -\frac{h^{0\prime}}{1 + \left(h^{0\prime}\right)^2}, \\ g_t^{\{2\}} &= \boldsymbol{g} \cdot \mathbf{e}^{\{2\}} = 0, \\ g_3 &= \boldsymbol{g} \cdot \mathbf{e}_3 = -\frac{1}{\sqrt{1 + \left(h^{0\prime}\right)^2}}. \end{aligned} \quad (1.13)$$

1.3. *Parameterization of spheroids*

We parameterize the ellipsoidal surface via the zenith $x^{\{1\}} = \vartheta$ and the azimuth $x^{\{2\}} = \varphi$:

$$\boldsymbol{X}(\vartheta, \varphi) = (\sin\vartheta\cos\varphi, \sin\vartheta\sin\varphi, c\cos\vartheta) \quad (1.14)$$

The tangent and normal vectors to the substrate are:

$$\mathbf{e}_1 = [\cos(\vartheta)\cos(\varphi), \cos(\vartheta)\sin(\varphi), -c\sin(\vartheta)], \quad \mathbf{e}_2 = [-\sin(\vartheta)\sin(\varphi), \sin(\vartheta)\cos(\varphi), 0],$$

$$\mathbf{e}_3 = \left[\frac{\sqrt{2}c\sin^2(\vartheta)\cos(\varphi)}{\sqrt{\sin^2(\vartheta)\left(-\left(\left(c^2-1\right)\cos(2\vartheta) - c^2 - 1\right)\right)}}, \frac{\sqrt{2}c\sin^2(\vartheta)\sin(\varphi)}{\sqrt{\sin^2(\vartheta)\left(-\left(\left(c^2-1\right)\cos(2\vartheta) - c^2 - 1\right)\right)}}, \right.$$
$$\left. \frac{\sqrt{2}\sin(\vartheta)\cos(\vartheta)}{\sqrt{\sin^2(\vartheta)\left(-\left(\left(c^2-1\right)\cos(2\vartheta) - c^2 - 1\right)\right)}} \right] \quad (1.15)$$

The metric tensor and the inverse metric tensor therefore read:

$$\begin{aligned} \mathbb{G}_{ij} = \mathbf{e}_i \cdot \mathbf{e}_j &= \begin{pmatrix} \frac{1}{2}\left(-\left(c^2-1\right)\cos(2\vartheta) + c^2 + 1\right) & 0 \\ 0 & \sin^2(\vartheta) \end{pmatrix}, \\ \mathbb{G}^{\{ij\}} = \mathbf{e}^{\{i\}} \cdot \mathbf{e}^{\{j\}} &= \begin{pmatrix} \frac{2}{-\left(c^2-1\right)\cos(2\vartheta)+c^2+1} & 0 \\ 0 & \csc^2(\vartheta) \end{pmatrix}. \end{aligned} \quad (1.16)$$

The curvature tensor is:

$$\mathbb{K}_i^{\{j\}} = \begin{pmatrix} -\frac{2\sqrt{2}c\sin^3(\vartheta)}{\left(\sin^2(\vartheta)\left(-\left(c^2-1\right)\cos(2\vartheta)+c^2+1\right)\right)^{3/2}} & 0 \\ 0 & -\frac{\sqrt{2}c\sin(\vartheta)}{\sqrt{\sin^2(\vartheta)\left(-\left(\left(c^2-1\right)\cos(2\vartheta)-c^2-1\right)\right)}} \end{pmatrix}, \quad (1.17)$$

from which the mean and Gaussian curvature are obtained:

$$\begin{aligned} \mathcal{K} &= \frac{\sqrt{2}c\sin^3(\vartheta)\left(\left(c^2-1\right)\cos(2\vartheta)-c^2-3\right)}{\left(\sin^2(\vartheta)\left(-\left(c^2-1\right)\cos(2\vartheta)+c^2+1\right)\right)^{3/2}}, \\ \mathcal{G} &= \frac{4c^2}{\left(-\left(c^2-1\right)\cos(2\vartheta)+c^2+1\right)^2}. \end{aligned} \quad (1.18)$$

The gravity components in the contravariant base read:

$$\begin{aligned} g_t^{\{1\}} &= \boldsymbol{g}\cdot\mathbf{e}^{\{1\}} = \frac{c\sin(\vartheta)}{c^2\sin^2(\vartheta)+\cos^2(\vartheta)}, \\ g_t^{\{2\}} &= \boldsymbol{g}\cdot\mathbf{e}^{\{2\}} = 0, \\ g_3 &= \boldsymbol{g}\cdot\mathbf{e}_3 = -\frac{\sqrt{2}\sin(\vartheta)\cos(\vartheta)}{\sqrt{\sin^2(\vartheta)\left(-\left(\left(c^2-1\right)\cos(2\vartheta)-c^2-1\right)\right)}}. \end{aligned} \quad (1.19)$$

Note that imposing $c = 1$ we recover the case of a sphere of unitary radius.

1.4. *Parameterization of tori*

We consider a torus of unitary tube radius and distance d between the center of the tube and the axis of revolution. The parameterization is performed using the colatitude $x^{\{1\}} = \vartheta$ and the azimuth $x^{\{2\}} = \varphi$:

$$\boldsymbol{X}(\vartheta,\varphi) = ((d+\sin\vartheta)\cos\varphi, (d+\sin\vartheta)\sin\varphi, \cos\vartheta) \quad (1.20)$$

The tangent and normal vectors to the substrate are:

$$\begin{aligned} \mathbf{e}_1 &= [\cos(\vartheta)\cos(\varphi), \cos(\vartheta)\sin(\varphi), -\sin(\vartheta)], \\ \mathbf{e}_2 &= [-(d+\sin(\vartheta))\sin(\varphi), (d+\sin(\vartheta))\cos(\varphi), 0], \\ \mathbf{e}_3 &= \left[\frac{\sin(\vartheta)\cos(\varphi)(d+\sin(\vartheta))}{d+\sin(\vartheta)}, \frac{\sin(\vartheta)\sin(\varphi)(d+\sin(\vartheta))}{d+\sin(\vartheta)}, \frac{\cos(\vartheta)(d+\sin(\vartheta))}{d+\sin(\vartheta)}\right]. \end{aligned} \quad (1.21)$$

The metric tensor and the inverse metric tensor read:

$$\begin{aligned} \mathbb{G}_{ij} &= \mathbf{e}_i\cdot\mathbf{e}_j = \begin{pmatrix} 1 & 0 \\ 0 & (d+\sin(\vartheta))^2 \end{pmatrix}, \\ \mathbb{G}^{\{ij\}} &= \mathbf{e}^{\{i\}}\cdot\mathbf{e}^{\{j\}} = \begin{pmatrix} 1 & 0 \\ 0 & \frac{1}{(d+\sin(\vartheta))^2} \end{pmatrix}. \end{aligned} \quad (1.22)$$

The curvature tensor is:

$$\mathbb{K}_i^{\{j\}} = \begin{pmatrix} -1 & 0 \\ 0 & -\frac{\sin(\vartheta)}{d+\sin(\vartheta))} \end{pmatrix}, \quad (1.23)$$

from which the mean and Gaussian curvature are obtained:

$$\begin{aligned}\mathcal{K} &= -\frac{d+2\sin(\vartheta)}{d+\sin(\vartheta)},\\ \mathcal{G} &= \frac{\sin(\vartheta)}{d+\sin(\vartheta)}.\end{aligned} \tag{1.24}$$

The gravity components read:

$$\begin{aligned}g_t^{\{1\}} &= \boldsymbol{g}\cdot\mathbf{e}^1 = \sin(\vartheta),\\ g_t^{\{2\}} &= \boldsymbol{g}\cdot\mathbf{e}^{\{2\}} = 0,\\ g_3 &= \boldsymbol{g}\cdot\mathbf{e}_3 = -\frac{\cos(\vartheta)(d+\sin(\vartheta))}{d+\sin(\vartheta)}.\end{aligned} \tag{1.25}$$

1.5. *Parameterization of ellipsoids*

We consider an ellipsoid of axes aR, bR and R, with the last one aligned along the vertical direction. The non-dimensionalization is performed by assuming as characteristic length the vertical axis R. The substrate is identified by:

$$\mathbf{X} = [a\sin(\vartheta)\cos(\varphi), b\sin(\vartheta)\sin(\varphi), \cos(\vartheta)] \tag{1.26}$$

The metric tensor reads:

$$\mathbb{G}_{ij} = \begin{pmatrix} \cos^2(\vartheta)\left(a^2\cos^2(\varphi)+b^2\sin^2(\varphi)\right)+\sin^2(\vartheta) & \left(b^2-a^2\right)\sin(\vartheta)\cos(\vartheta)\sin(\varphi)\cos(\varphi) \\ \left(b^2-a^2\right)\sin(\vartheta)\cos(\vartheta)\sin(\varphi)\cos(\varphi) & \sin^2(\vartheta)\left(a^2\sin^2(\varphi)+b^2\cos^2(\varphi)\right) \end{pmatrix}, \tag{1.27}$$

while the components of the inverse metric tensor are:

$$\begin{aligned}\mathbb{G}^{\{11\}} &= \frac{a^2\sin^2(\varphi)+b^2\cos^2(\varphi)}{\sin^2(\vartheta)\left(a^2\sin^2(\varphi)+b^2\cos^2(\varphi)\right)+a^2b^2\cos^2(\vartheta)},\\ \mathbb{G}^{\{12\}} &= \mathbb{G}^{\{21\}} = \frac{\left(a^2-b^2\right)\cot(\vartheta)\sin(\varphi)\cos(\varphi)}{\sin^2(\vartheta)\left(a^2\sin^2(\varphi)+b^2\cos^2(\varphi)\right)+a^2b^2\cos^2(\vartheta)},\\ \mathbb{G}^{\{22\}} &= \left(\csc^2(\vartheta)\left(a^2\cot^2(\vartheta)\cos^2(\varphi)+b^2\cot^2(\vartheta)\sin^2(\varphi)+1\right)\right)/\left(a^2b^2\cot^2(\vartheta)\cos^4(\varphi)\right.\\ &\quad \left.+a^2\sin^2(\varphi)\left(b^2\cot^2(\vartheta)\sin^2(\varphi)+1\right)+b^2\cos^2(\varphi)\left(2a^2\cot^2(\vartheta)\sin^2(\varphi)+1\right)\right).\end{aligned} \tag{1.28}$$

The mean and gaussian curvatures read:

$$\mathcal{K} = -\frac{ab\left[3\left(a^2+b^2\right)+2+\left(a^2+b^2-2\right)\cos(2\vartheta)-2\left(a^2-b^2\right)\cos(2\varphi)\sin^2\vartheta\right]}{4\left[a^2b^2\cos^2\vartheta+\left(b^2\cos^2\varphi+a^2\sin^2\varphi\right)\sin^2\vartheta\right]^{3/2}} \tag{1.29}$$

$$\mathcal{G} = \frac{a^2b^2}{\left[a^2b^2\cos^2\vartheta+\left(b^2\cos^2\varphi+a^2\sin^2\varphi\right)\sin^2\vartheta\right]^2} \tag{1.30}$$

The gravity components in the contravariant base read:

$$g_t^{\{1\}} = \frac{\sin(\vartheta)\left(a^2\sin^2(\varphi)+b^2\cos^2(\varphi)\right)}{\sin^2(\vartheta)\left(a^2\sin^2(\varphi)+b^2\cos^2(\varphi)\right)+a^2b^2\cos^2(\vartheta)}, \tag{1.31}$$

$$g_t^{\{2\}} = \frac{\sin(\varphi)\cos(\varphi)\left(a^2\cos(\vartheta)-b^2\cos(\vartheta)\right)}{a^2b^2\cos^2(\vartheta)\cos^2(\varphi)+a^2b^2\cos^2(\vartheta)\sin^2(\varphi)+a^2\sin^2(\vartheta)\sin^2(\varphi)+b^2\sin^2(\vartheta)\cos^2(\varphi)}, \tag{1.32}$$

$$g_3 = -\frac{ab\sin(\vartheta)\cos(\vartheta)}{\sqrt{\sin^4(\vartheta)\left(a^2\sin^2(\varphi)+b^2\cos^2(\varphi)\right)+a^2b^2\sin^2(\vartheta)\cos^2(\vartheta)}}. \tag{1.33}$$

2. Classical drainage and spreading solutions: diverging flow on a sphere, a cylinder and a cone

We consider the coating of an initially uniform layer of fluid on a sphere of radius R, recently analyzed by Takagi & Huppert (2010); Lee *et al.* (2016) and Qin *et al.* (2021). In non-dimensional form, the parameterization of the spherical surface through the zenith (or colatitude) $x^{\{1\}} = \vartheta$ and azimuth $x^{\{2\}} = \varphi$ reads:

$$\boldsymbol{X}(\vartheta,\varphi) = (\sin\vartheta\cos\varphi, \sin\vartheta\sin\varphi, \cos\vartheta) \tag{2.1}$$

The gravity components tangent to the substrate and w respectively read:

$$g_t^{\{1\}}(\vartheta) = \sin(\vartheta), \quad g_t^{\{2\}} = 0, \quad w(\vartheta) = \sin(\vartheta). \tag{2.2}$$

The drainage problem can be written as follows:

$$\frac{\partial h(\vartheta,t)}{\partial t} + \frac{1}{3w(\vartheta)}\frac{\partial}{\partial\vartheta}\left(g_t^{\{1\}}(\vartheta)w(\vartheta)h(\vartheta,t)^3\right) = 0 \rightarrow \frac{\partial h}{\partial t} + \frac{1}{3\sin(\vartheta)}\frac{\partial}{\partial\vartheta}\left(\sin^2(\vartheta)h^3\right) = 0. \tag{2.3}$$

The problem admits a large-time solution by separation of variables, independent of the initial condition (Couder *et al.* 2005; Qin *et al.* 2021):

$$h(z,t) = \eta(z)t^{-1/2}, \quad z = \cos(\vartheta), \tag{2.4}$$

where

$$\eta(z) = \frac{[f(1)-f(z)]^{1/2}}{\left(1-z^2\right)^{1/3}}, \quad f(z) = z\mathrm{Hy}\left(\frac{1}{3},\frac{1}{2};\frac{3}{2};z^2\right), \tag{2.5}$$

where Hy is the hypergeometric function. Takagi & Huppert (2010), with a scaling analysis around the pole, found that $h \approx \sqrt{\frac{3}{4}}t^{-1/2}$. A more formal approach which gives the solution at different orders in ϑ for a generic initial condition, was proposed by Lee *et al.* (2016) through an asymptotic expansion of equation (2.3) around the pole, i.e. $h(\vartheta,t) = H_0(t) + \vartheta H_1(t) + \vartheta^2 H_2(t) + ...$, leading to the following solution, truncated at $O(\vartheta^2)$:

$$h(\vartheta,t) \approx \frac{1}{\sqrt{1+\frac{4}{3}t}}\left[1+\frac{\vartheta^2}{10}\left(1+C\left(1+\frac{4}{3}t\right)^{-5/2}\right)\right]+O(\vartheta^4), \tag{2.6}$$

where the constant C depends on the initial condition. Note that the odd terms in the asymptotic expansion are zero because of the symmetry with respect to $\vartheta = 0$. When $t \rightarrow \infty$,

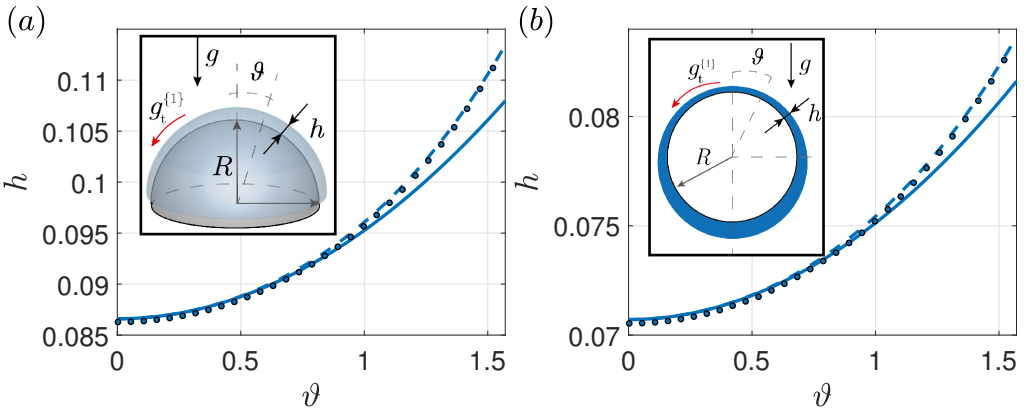

Figure 1: (a) Coating on a sphere: film thickness as a function of the zenith ϑ at $t = 100$, numerical simulation (dots), large-time analytical solution at order $O(1)$ (red dashed line), $O(\vartheta^2)$ (solid line) and $O(\vartheta^6)$ (blue dashed line). (b) Coating on a cylinder: film thickness as a function of the zenith ϑ at $t = 300$, numerical simulation (dots), large-time analytical solution at order $O(1)$ (red dashed line), $O(\vartheta^2)$ (solid line) and $O(\vartheta^6)$ (blue dashed line).

the term that multiplies C vanishes, at the leading order. The leading-order large-time solution at order $O(\vartheta^6)$ reads:

$$h(\vartheta, t) = \sqrt{\frac{3}{4t}}\left(1 + \frac{\vartheta^2}{10} + \frac{41\vartheta^4}{4800} + \frac{1187\vartheta^6}{1584000}\right) + O(\vartheta^8) + O\left(\frac{1}{t^{3/2}}\right). \tag{2.7}$$

The large-time solution is thus independent of the initial condition and has a time dependence analogous to the one obtained by Takagi & Huppert (2010) and Qin *et al.* (2021). The resulting zenith dependence is also an approximation of the hypergeometric function. In figure 1(a), the various orders large-time analytical solutions show a good agreement with the numerical solution of equation (2.3).

We now consider the case of the spreading on a sphere (of radius R) of an initial mass of fluid of thickness $h_i = 1$, contained in the region $\vartheta < \vartheta_0$, $0 < \varphi < 2\pi$. Substituting the $O(\vartheta)$ approximation of equation (2.6) and $w \approx \vartheta$ into the conservation of mass (equation (3.13) of the manuscript), one finds the following expressions for the front angle $\vartheta_F(t)$ and the thickness at the front $h_F(\vartheta(t))$:

$$\frac{\vartheta_F}{\vartheta_0} = \left(\frac{4}{3}t\right)^{1/4}, \quad h_F = \left(\frac{\vartheta_0}{\vartheta_F}\right)^{1/2}, \tag{2.8}$$

which is the non-dimensional version of the results reported in Takagi & Huppert (2010).

In the case of the coating on a cylinder of radius R, the non-dimensional parameterization reads:

$$\boldsymbol{X} = (\sin\vartheta, y, \cos\vartheta), \tag{2.9}$$

The tangential gravity component and w read:

$$g_t^{\{1\}} = \sin(\vartheta), \quad g_t^{\{2\}} = 0, \quad w = 1. \tag{2.10}$$

The drainage problem reads:

$$\frac{\partial h}{\partial t} + \frac{1}{3}\frac{\partial}{\partial \vartheta}\left(\sin(\vartheta)h^3\right) = 0. \tag{2.11}$$

Performing an asymptotic expansion around the pole in powers of ϑ, the large-time solution

reads (Balestra *et al.* 2019):

$$h(\vartheta,t)=\sqrt{\frac{3}{2t}}\left(1+\frac{\vartheta^2}{16}+\frac{43\vartheta^4}{10752}+\frac{109\vartheta^6}{368640}\right)+O(\vartheta^8)+O\left(\frac{1}{t^{3/2}}\right), \tag{2.12}$$

whose $O(1)$ approximation correspond to the result of Takagi & Huppert (2010). Note that the large-time solution is independent of the initial condition, and is in good agreement with the numerical solution of equation (2.11) (see figure 1(*b*)). Takagi & Huppert (2010) also studied the spreading on a cylinder. Following the same steps adopted for the case of the sphere, one obtains the following expressions for the front angle and thickness:

$$\frac{\vartheta_F}{\vartheta_0}=\left(\frac{2t}{3}\right)^{1/2},\quad h_F=\frac{\vartheta_0}{\vartheta_F}. \tag{2.13}$$

We conclude by considering the classical problem of the coating on a conical substrate, of maximum radius R and height aR. This problem is typically solved by employing a self-similar approach. A large-time solution can be obtained, similar to Qin *et al.* (2021) for the sphere coating. We consider a parameterization in cylindrical coordinates (see ESM for further details), which reads, in non-dimensional form:

$$\boldsymbol{X}=(r\cos\varphi, r\sin\varphi, -ar), \tag{2.14}$$

where r is the radius and φ is the azimuth. In this parameterization, the gravity terms and w read:

$$g_t^{\{1\}}=\frac{a}{a^2+1},\quad g_t^{\{2\}}=0,\quad w(r)=\sqrt{(a^2+1)}r \tag{2.15}$$

The lubrication equation reads:

$$\frac{\partial h(r,t)}{\partial t}+\frac{1}{3\sqrt{(a^2+1)}r}\frac{\partial}{\partial r}\left(\sqrt{(a^2+1)}r\, g_t^{\{1\}}(r)h(r,t)^3\right)=0 \tag{2.16}$$

Developing the derivatives, one obtains:

$$\frac{\partial h}{\partial t}+\frac{ah^2}{a^2+1}\frac{\partial h}{\partial r}+\frac{ah^3}{3a^2r+3r}=0, \tag{2.17}$$

which is completed with the initial condition $h(r,0)=1$. This problem admits a self-similar solution of the form $h(r,t)=f(\eta)$, where $\eta=t/r$ is the self-similar variable. By substituting the self-similar ansatz in equation (2.17), one obtains the following ordinary differential equation:

$$f'\left(1-\frac{a}{1+a^2}\eta f^2\right)+\frac{1}{3}\frac{a}{1+a^2}f^3=0,\quad f(0)=1, \tag{2.18}$$

which can be numerically solved so as to find the solution of the initial value problem. The results are reported in figure 2. Moreover,the following expression satisfies equation (2.18):

$$f(\eta)=f_0\eta^{-1/2},\quad f_0=\sqrt{\frac{3(a^2+1)}{5a}}\rightarrow h(r,t)=\sqrt{\frac{3(a^2+1)}{5a}}\sqrt{\frac{r}{t}}. \tag{2.19}$$

The latter expression is well known in literature (Acheson 1990) and well agrees with the numerical self-similar solution as $\eta\rightarrow\infty$, i.e. $t\rightarrow\infty$ or $r\rightarrow 0$ (see figure 2). The large-time solution is thus independent of the initial condition.

In analogy to the previous cases, the spreading of an initial mass of fluid of height $h_i=1$

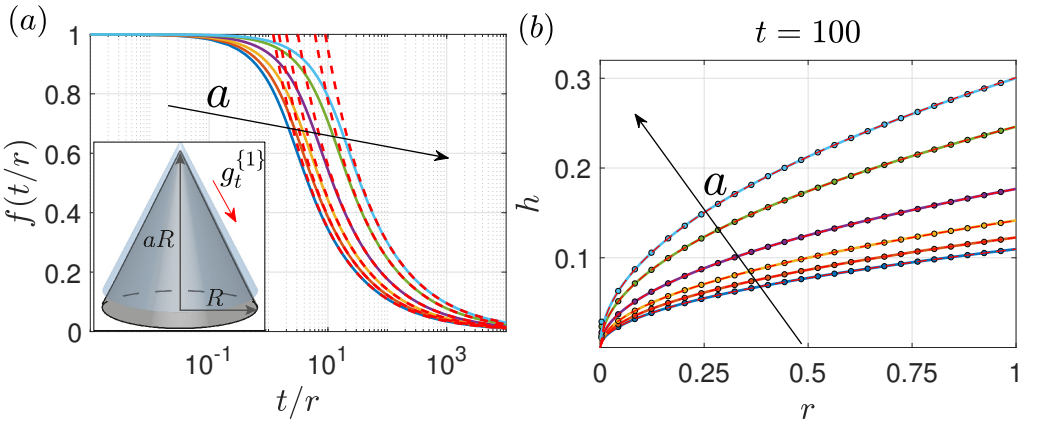

Figure 2: (a) Self-similar solution for the coating of a cone $h(r,t) = f(\eta)$ as a function of $\eta = t/r$, for different values of a. The red dashed lines denote the corresponding large-time approximation. (b) Comparison at $t = 100$ between the numerical (colored dots) self-similar (solid lines) and large-time (red dashed lines) solutions. The different colors correspond to $a = 1$ (blue), $a = 2$ (orange), $a = 3$ (yellow), $a = 5$ (purple), $a = 10$ (green), $a = 15$ (cyan).

contained in a region $r < r_0$ can be solved by employing the large-time solution: (2.19):

$$h(r,t) = \sqrt{\frac{3(a^2+1)}{5a}}\sqrt{\frac{r}{t}}, \quad w(r) = \sqrt{(a^2+1)}r. \tag{2.20}$$

Upon integration in $0 < \varphi < 2\pi$ and $0 < r < r_N$, one obtains the radial position of the front r_N:

$$r_N = \left(\frac{125V^2}{48\pi^2}\frac{a}{(a^2+1)^2}\right)^{1/5} t^{1/5}, \tag{2.21}$$

where $V = \pi r_0^2\sqrt{a^2+1}$ is the initial volume. Noting that $\frac{a}{(a^2+1)^2} = \sin^3(\beta)\cos(\beta)$, where β is the inclination angle of the cone and the spreading distance from the tip of the cone is $s_N = r_N/\sin(\beta)$, one obtains the classical result for the spreading on a cone (Acheson 1990):

$$s_N = \left(\frac{125V^2}{48\pi^2}\frac{\cos\beta}{\sin^2\beta}\right)^{1/5} t^{1/5}, \tag{2.22}$$

3. Spreading and drainage on a paraboloid

3.1. *Drainage problem*

In this section, we consider the coating of a paraboloid of characteristic radial extent R. We parameterize the paraboloidal surface as follows:

$$\boldsymbol{X} = (r\cos\varphi, r\sin\varphi, -er^2) \tag{3.1}$$

The gravity term $g_t^{\{1\}}$ and w now read:

$$g_t^{\{1\}}(r) = \frac{2er}{4e^2r^2+1}, \quad w(r) = r\sqrt{4e^2r^2+1} \tag{3.2}$$

The lubrication equation reads:

$$\frac{\partial h}{\partial t} + \frac{2erh^2}{4e^2r^2+1}\frac{\partial h}{\partial r} + \frac{4\left(2e^3r^2+e\right)h^3}{3\left(4e^2r^2+1\right)^2} = 0. \tag{3.3}$$

In analogy with the sphere case, we expand the solution in series of r:

$$h(r,t) = H_0(t) + r^2H_2(t) + r^4H_4(t) + r^6H_6(t) + \ldots \tag{3.4}$$

Because of symmetry, all the odd terms in r are zero. In Appendix **??** we report the analytical developments. The solution at order $O(r^6)$, for $t \to \infty$, reads:

$$h(r,t) = \frac{\sqrt{\frac{3}{2}}\sqrt{\frac{1}{t}}\left(3248e^6r^6 - 1540e^4r^4 + 1650e^2r^2 + 1375\right)}{2750\sqrt{e}} + O(r^8) + O\left(\frac{1}{t^{3/2}}\right). \tag{3.5}$$

Also in this case, $H_0 = \left(\frac{3}{2\mathcal{K}_p t}\right)^{1/2}$, where $\mathcal{K}_p = 4e$ is the absolute value of the mean curvature at the top.

Equation (3.3) is solved in the domain $0 < r < 1$ with initial condition $h(0,t) = 1$. Numerical convergence for all values of e is achieved with a characteristic element size $\Delta r = 0.01$.

The comparison between the analytical and numerical drainage solution is reported in figure 3(a). The solution is characterized by mild variations of the thickness with the radius. The comparison shows a good agreement for $e < 1$, while already at $e = 1$ the accuracy of the analytical solution rapidly degrades as $r > 0.5$.

An analytical approximation for larger values of e can be obtained by assuming $er \gg 1$ in equation (3.3):

$$\frac{\partial h}{\partial t} + \frac{h^2}{2er}\frac{\partial h}{\partial r} + \frac{h^3}{6er^2} = 0, \quad h(r,0) = 1. \tag{3.6}$$

The problem admits a self-similar solution of the form $h(r,t) = f(\xi)$, where $\xi = t/r^2$. Following the same procedure of the cone problem, one obtains the following ordinary differential equation:

$$f'\left(1 - \frac{1}{e}\xi f^2\right) + \frac{1}{6e}f^3 = 0, \quad f(0) = 1. \tag{3.7}$$

The resulting equation is formally analogous to the self-similar problem of the cone (2.18), with different coefficients. The numerical solution is reported in figure 3(b). We find an approximate solution of the form $f(\xi) = f_0\xi^{-1/2}$, where $f_0 = \sqrt{3e}/2$:

$$h(r,t) = \frac{\sqrt{3e}}{2}\frac{r}{\sqrt{t}}, \tag{3.8}$$

that well agrees with the solution of the self-similar initial value problem for $\xi \to \infty$, i.e. $t \to \infty$ (see red dashed lines in 3(b)). The agreement with the numerical solution for $e > 2$, shown in figure 3(c) is very good, except in the close vicinity of $r = 0$, in which the expansion of equation (3.5) can be employed.

Following the reasoning of Section 3.1 of the manuscript, the mean curvature decreases moving downstream, therefore inducing film thickening. Also the tangential gravity component increases, thus leading to an overall film thickening effect. Interestingly, the drainage problem was approached by employing the asymptotic expansion, the self-similar solution and the large-time scaling arguments.

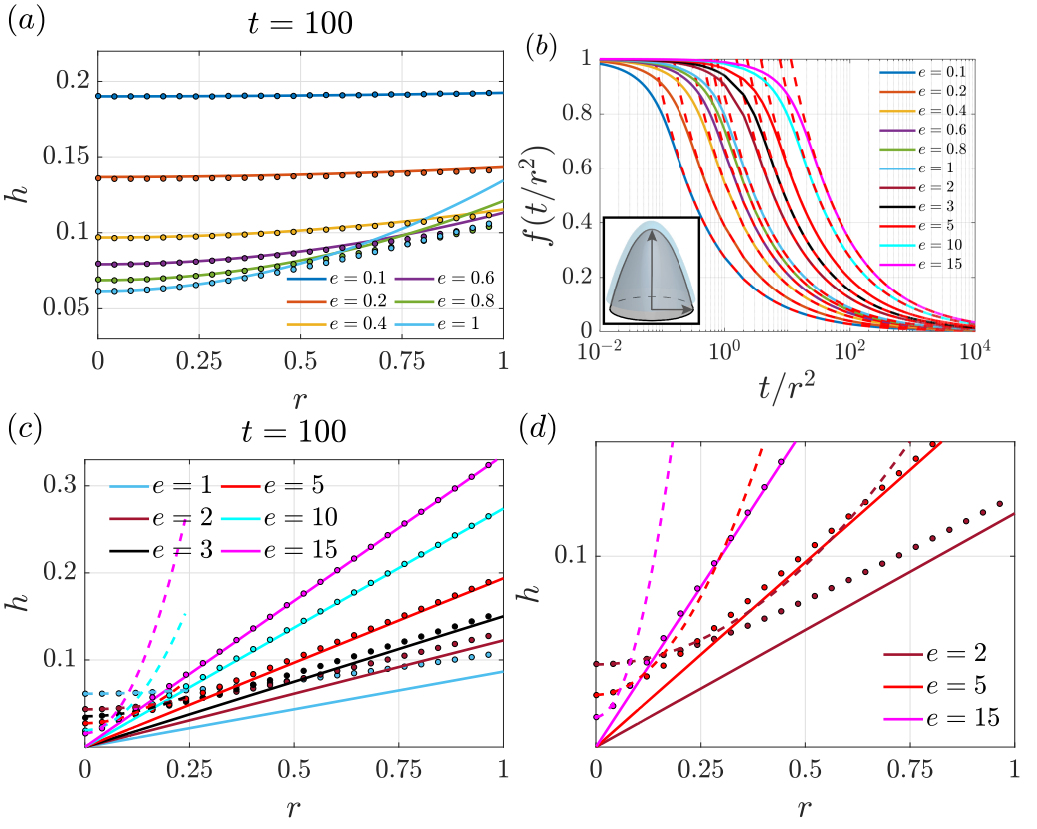

Figure 3: (a) Comparison of the analytical solution (equation (3.5), solid lines) against the numerical one (colored dots) for the drainage on a paraboloid. (b) Self-similar solution for the coating on a paraboloid, valid for $er \gg 1$ (colored lines). The red dashed lines are the corresponding large-time approximations (equation (3.8)). (c) Comparison of the numerical solution (colored dots) with the self-similar one for $er \gg 1$ (solid lines). The dashed lines denote the $O(r^6)$ approximation of equation (3.5). (d) Zoom in (c) to highlight the range of validity of the two analytical solutions.

3.2. *Spreading problem*

We now focus on the spreading problem of a mass of fluid of initial thickness $h_i = 1$ contained in the region $r < r_0$. The conservation of mass reads:

$$\int_0^{2\pi}\int_0^{r_F(t)} h(r,t)w(r)\mathrm{d}r\mathrm{d}\varphi = \int_0^{2\pi}\int_0^{r_0} w(r)\mathrm{d}r\mathrm{d}\varphi \rightarrow \int_0^{r_F(t)} h(r,t)w(r)\mathrm{d}r = \int_0^{r_0} w(r)\mathrm{d}r, \tag{3.9}$$

where $w(r)$ is given by equations (3.2). The thickness $h(r,t)$ is given by the two large-time analytical solutions (3.5), valid for small values of e, and (3.8), valid instead when large values of e are considered, far from the pole. The resulting problems for the front radius r_F and thickness h_F are numerically solved via the built-in function "fsolve" in Matlab, and the results are reported in figure 4, for the two different analytical solutions. These results are compared with following two analytical approximations in the vicinity of ($r \ll 1$) and far from the pole ($er \gg 1$). When small values of r and large times are considered, the thickness

and w can be approximated as follows:

$$h = \sqrt{\frac{3}{8et}} + O(r^2) + O\left(\frac{1}{t^{3/2}}\right), \quad w = r + O(r^2). \tag{3.10}$$

Substituting in equation (3.9) and keeping at most $O(r)$ terms, one obtains the front radius and thickness:

$$r_F = r_0 \left(\frac{8et}{3}\right)^{1/4}, \quad h_F = \left(\frac{r_0}{r_F}\right)^2, \tag{3.11}$$

which well compares with the numerical solutions of the implicit relation (3.9) (see figure 4(a, b)).

The same analytical developments can be employed for the case $er \gg 1$ and $t \to \infty$:

$$h = \frac{\sqrt{3e}}{2}\frac{r}{\sqrt{t}}, \quad w = r\sqrt{4e^2r^2 + 1} \approx 2er^2, \tag{3.12}$$

which leads to:

$$r_F = \left(\frac{8}{3}\sqrt{\frac{t}{3e}}r_0^3\right)^{1/4}, \quad h_F = \frac{4}{3}\left(\frac{r_0}{r_F}\right)^3. \tag{3.13}$$

Also in this case, a good agreement is observed (see figure 4(c, d)). The agreement improves when larger values of e at larger r are considered. We finally compare these theoretical results with two numerical simulations of the complete model (equation (2.5) of the manuscript). To impose the outlet condition, we consider the domain $0 < r < 3$ and employ a Sponge method to relax the thickness to zero avoiding reflections from the outlet (Högberg & Henningson 1998; Lerisson *et al.* 2020). Equation (3.3) is thus modified as follows to impose the Sponge condition:

$$\frac{\partial h}{\partial t} + \frac{2erh^2}{4e^2r^2+1}\frac{\partial h}{\partial r} + \frac{4\left(2e^3r^2+e\right)h^3}{3\left(4e^2r^2+1\right)^2} = -\frac{h}{2}\left(1 + \tanh\left(\eta_{sp}\left(r - r_{sp}\right)\right)\right) = -h\mathrm{Sp}(r), \tag{3.14}$$

where $\eta_{sp} = 3$ and $r_{sp} = 2.7$, and initial condition $h(0, t) = 1 - \mathrm{Sp}(r)$. The numerical results show a good agreement with the prediction of the front position and thickness.

REFERENCES

Acheson, DJ 1990 *Elementary fluid dynamics: Oxford University Press*. Oxford, England.

Balestra, G., Badaoui, M., Ducimetière, Y-M & Gallaire, F. 2019 Fingering instability on curved substrates: optimal initial film and substrate perturbations. *Journal of Fluid Mechanics* **868**, 726–761.

Couder, Y., Fort, E., Gautier, C.-H. & Boudaoud, A. 2005 From bouncing to floating: Noncoalescence of drops on a fluid bath. *Phys. Rev. Lett.* **94**, 177801.

Högberg, M. & Henningson, D. 1998 Secondary instability of cross-flow vortices in falkner–skan–cooke boundary layers. *Journal of Fluid Mechanics* **368**, 339–357.

Lee, A., Brun, P-T, Marthelot, J., Balestra, G., Gallaire, F. & Reis, P. M. 2016 Fabrication of slender elastic shells by the coating of curved surfaces. *Nature communications* **7** (1), 1–7.

Lerisson, G., Ledda, P. G., Balestra, G. & Gallaire, F. 2020 Instability of a thin viscous film flowing under an inclined substrate: steady patterns. *Journal of Fluid Mechanics* **898**, A6.

Qin, J., Xia, Y-T & Gao, P. 2021 Axisymmetric evolution of gravity-driven thin films on a small sphere. *Journal of Fluid Mechanics* **907**.

Takagi, D. & Huppert, H. E. 2010 Flow and instability of thin films on a cylinder and sphere. *Journal of Fluid Mechanics* **647**, 221–238.

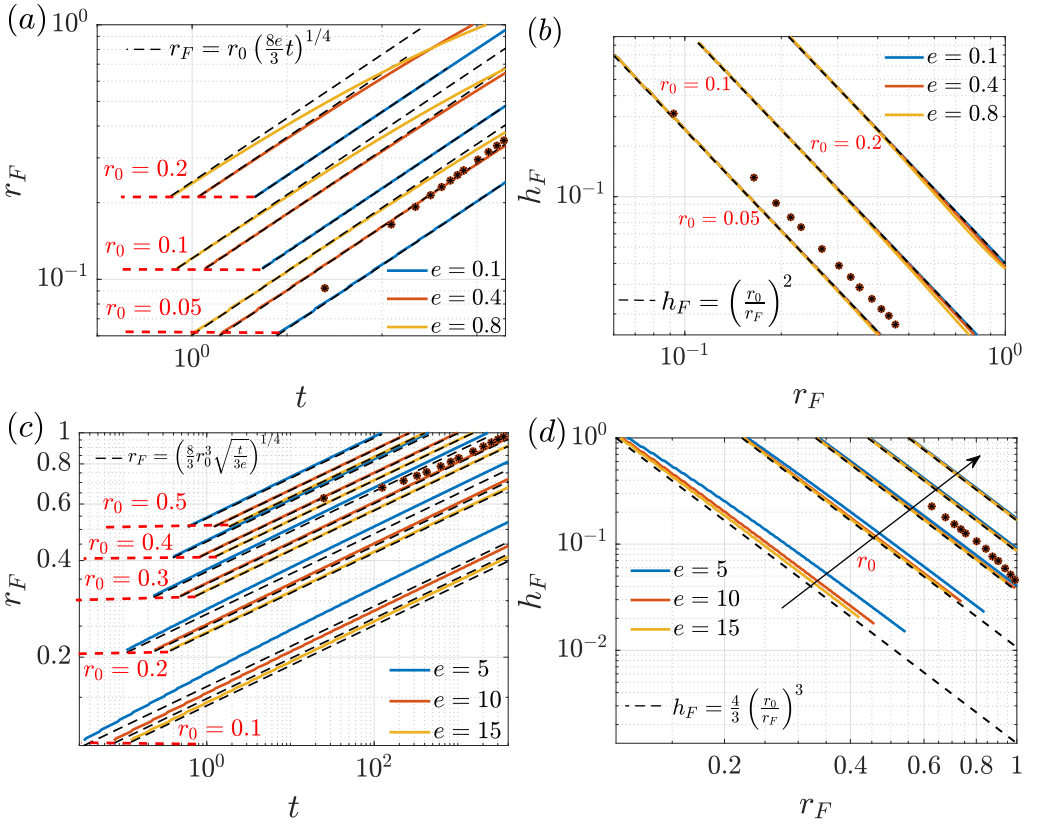

Figure 4: Spreading of an initial volume of fluid on an paraboloid. (a, c) Variation of the front angle ϑ_F with time and (b, d) of the thickness at the front h_F with ϑ_F, for different values of the initial angle ϑ_0 and e, for the (a, b) asymptotic and (c, d) self-similar solution. The solid and dot-dashed lines denote the values of ϑ_F and h_F on the outer and inner sides, respectively. The black dashed lines correspond to the analytical approximations of the relation $\vartheta_F(t)$ and $h_F(\vartheta_F)$, respectively, while the stars are the values recovered by a numerical simulation of the complete model with (a, b) $e = 0.8$, $Bo = 5000$, $\delta = 10^{-3}$, $h_{pr} = 0.0025$ and (c, d) $e = 10$, $Bo = 100$, $\delta = 10^{-2}$, $h_{pr} = 0.0025$.